

Efficient bulk mass accommodation and dissociation of N₂O₅ in neutral aqueous aerosol

Goran Gržinić^{1,2}, Thorsten Bartels-Rausch¹, Andreas Türler^{2,3}, Markus Ammann²

¹ Laboratory of Environmental Chemistry, Paul Scherrer Institut, Villigen, 5232, Switzerland

² Department of Chemistry and Biochemistry, University of Bern, Bern, 3012, Switzerland

³ Laboratory of Radiochemistry, Paul Scherrer Institut, Villigen, 5232, Switzerland

Correspondence to: Markus Ammann (markus.ammann@psi.ch)

Abstract. An isotope exchange experiment with the short-lived radioactive tracer ¹³N is used to trace N₂O₅ uptake into nitrate containing aqueous aerosol particles. While uptake of ¹³N labelled N₂O₅ to deliquesced Na₂SO₄ aerosol is consistent with previous studies, in presence of aerosol phase nitrate efficient exchange of labelled nitrate with the non-labelled nitrate pool was observed. The experiments provide direct evidence for efficient bulk mass accommodation of N₂O₅ into aqueous solution with $\alpha_b > 0.4$ at room temperature, as well as for the fast dissociation into nitronium and nitrate. While for experimental reasons this study is limited to non-acidic nitrate containing aerosol, it is likely that bulk mass accommodation and dissociation are not limiting N₂O₅ uptake also under wider ranges of conditions.

1 Introduction

The central role of NO_x in the regulation of the oxidative capacity of the atmosphere is well established. N₂O₅, an important species of the nighttime chemistry of nitrogen oxides, has been identified as one of the major reservoir species and potential sinks of NO_x (Abbatt et al., 2012; Chang et al., 2011). NO₂ reacts with O₃ to form NO₃, which then react together to form N₂O₅ (R1).

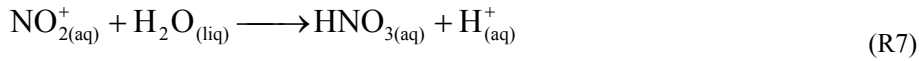


Depending on location N₂O₅ may be removed primarily by heterogeneous hydrolysis to nitric acid or other products on aerosol surfaces, providing thus a nighttime sink for atmospheric NO_x (R2) (Abbatt et al., 2012; Chang et al., 2011).



Removal of N₂O₅ leads to a reduction of atmospheric NO_x and consequent reduction of tropospheric ozone and thus the oxidative capacity of the atmosphere (Dentener and Crutzen, 1993; Evans and Jacob, 2005). The reactivity of N₂O₅ with aerosols has been of ongoing interest for the past two decades. Laboratory investigations have encompassed measurement of uptake kinetics to a wide array of inorganic aerosols, like H₂SO₄/sulphates (Hallquist et al., 2003; Hanson and Lovejoy, 1994), NaCl/marine aerosol (Gaston and Thornton, 2016; George et al., 1994; Thornton and Abbatt, 2005), nitrate containing inorganic aerosol (Hallquist et al., 2003; Mentel et al., 1999; Wahner et al., 1998) and mineral dust (Karagulian et al., 2006; Wagner et al., 2008). Further constraints have also been derived from field observations of N₂O₅ and aerosol abundance and composition (Bertram et al., 2009; Phillips et al., 2016). The uptake coefficient γ (defined as the probability that a gas kinetic collision of a molecule leads to its uptake at the interface) on deliquesced inorganic aerosol is in the 10⁻¹-10⁻² range. Organic aerosol on the other hand presents a wider range of

reactivities, with values approaching those of inorganic aerosols in certain cases such as for malonic acid (Griffiths et al., 2009; Thornton et al., 2003) at around 10^{-2} , while in other cases the uptake coefficients go down to 10^{-3} - 10^{-5} , such as for some polycarboxilic acids like citric acid (Gržinić et al., 2015), succinic acid or humic acid (Badger et al., 2006; Griffiths et al., 2009), long chained fatty acids and polyalcohols (Gross et al., 2009) that indicate varying effects of water content and viscosity on the reactivity and kinetic regime. Additionally, coating aqueous particles with insoluble organic films has shown to have an inhibiting effect on N_2O_5 uptake (Anttila et al., 2006; Folkers et al., 2003) by restricting transport from the gas phase to the aerosol phase, reduced solubility in the organic phase or limited water availability. The hydrolysis of $\text{N}_2\text{O}_5(\text{g})$ is believed to proceed through a multistep process (Behnke et al., 1997; Mozurkewich and Calvert, 1988): molecular solvation (R3) is followed by dissociation into nitronium (NO_2^+ , or its hydrated form H_2ONO_2^+) and nitrate (R4) with a rate coefficient, k_4 , estimated between 10^5 s^{-1} and 10^7 s^{-1} (Mentel et al., 1999; Bertram and Thornton, 2009; Griffiths et al., 2009). The fate of nitronium is governed by competition between the reaction with nitrate to yield molecular N_2O_5 again (R5) with a nearly collision limited rate coefficient, k_5 , of $2.4 \times 10^{10} \text{ M}^{-1} \text{ s}^{-1}$ (Mentel et al., 1999), the reaction with $\text{H}_2\text{O}(\text{l})$ to yield HNO_3 (R7) (k_5 , between 10^7 and $10^9 \text{ M}^{-1} \text{ s}^{-1}$ (Mentel et al., 1999; Behnke et al., 1997)) or reactions with other nucleophiles (such as chloride ion) not considered further here.



The elementary reactions constituting this mechanism have been suggested based on the kinetic behavior as a function of a range of conditions, but have not been unambiguously been proven by detecting, e.g., NO_2^+ directly. As long as nitrate is a minority species in the aerosol phase, the loss of N_2O_5 is driven by reaction R7. Depending on the water content, either the transfer of N_2O_5 into the aqueous phase, R3, also referred to as mass or bulk accommodation, the dissociation (R4) or R7 are rate limiting according to current understanding (Abbatt et al., 2012).

On the other hand, in presence of significant amounts of nitrate in the aqueous phase, the loss of nitronium ion by reaction with nitrate back to N_2O_5 , R5, becomes significant, and the uptake of N_2O_5 becomes lower with increasing nitrate content in the aerosol phase, typically by an order of magnitude. This effect is referred to as the ‘nitrate effect’ (Abbatt et al., 2012; Bertram and Thornton, 2009; Hallquist et al., 2003; Mentel et al., 1999; Wahner et al., 1998).

Most studies conducted related to N_2O_5 reactivity with aqueous aerosol so far were based on measuring the net gas-phase loss of N_2O_5 due to uptake on an aerosol. The kinetics were described with a simplified lumped mechanism by assigning an effective Henry’s law constant, H , of N_2O_5 of about 2 to 5 M atm^{-1} at room temperature and a net rate coefficient for the overall reaction of N_2O_5 with H_2O to HNO_3 , k_0^{II} , of around $10^5 \text{ M}^{-1} \text{ s}^{-1}$ (Ammann et al., 2013; Bertram and Thornton, 2009; Griffiths et al., 2009), so that the uptake coefficient can be described via the resistor model as given by equation (1).

$$\frac{1}{\gamma} = \frac{1}{\alpha_b} + \frac{c}{4HRT \sqrt{D_l k'' [\text{H}_2\text{O}] [\coth(r/l) - (l/r)]}} \quad l = \sqrt{\frac{D_l}{k'' [\text{H}_2\text{O}]}} \quad (1)$$

Where α_b denotes the bulk mass accommodation coefficient, c the mean thermal velocity of N_2O_5 in the gas phase, D_l the diffusion coefficient of N_2O_5 in the aqueous phase, usually set to $10^{-5} \text{ cm}^2 \text{ s}^{-1}$ for low viscosity aqueous aerosol, $[\text{H}_2\text{O}]$ the concentration of H_2O in M, r the particle radius and l the reacto-diffusive length. The apparent levelling off of γ towards high relative humidity was explained by a limiting α_b of about 0.03 (Ammann et al., 2013) or by introducing a dependence of the dissociation rate, k_4 , on the water content, leading to an apparent water content dependence of k_0^{II} (Bertram and Thornton, 2009). The effect of nitrate as mentioned above has been taken into account by using equation (2) instead of a fixed rate coefficient k_0^{II} :

$$k'' = k_0'' \left(1 - \frac{1}{1 + \frac{k_7 [\text{H}_2\text{O}]}{k_5 [\text{NO}_3^-]}} \right) \quad (2)$$

This expression requires the knowledge of the concentrations of water and nitrate and the ratio of the two rate coefficients k_7/k_5 , for which values between 0.02 and 0.06 lead to reasonable consistency with available data (Ammann et al., 2013; Bertram and Thornton, 2009). However, the actual size of the pool of dissolved N_2O_5 (or its dissociated products NO_2^+ and NO_3^-), the true value of the bulk mass accommodation coefficient, α_b , and the rate coefficients for the individual reactions remained elusive. In this study, we make specific use of the short-lived radioactive isotope ^{13}N (Ammann, 2001; Gržinić et al., 2015; Gržinić et al., 2014) to trace the exchange of ^{13}N -labelled nitrate resulting from uptake of labelled N_2O_5 with the non-labelled nitrate pool in the aerosol phase. This allows obtaining a direct estimate of α_b and constraints for the N_2O_5 dissociation (R4) and the recombination reaction (R5). The tracer method is very sensitive in detecting phase transfer of labelled N_2O_5 at very low gas phase concentrations and thus is able to escape any artefact nitrate effect due to build-up of nitrate during the course of a kinetic experiment for experiments with aerosol without any nitrate initially as discussed by Gržinić et al. (2015). However, this sensitivity comes at the expense of chemical selectivity in the sense that re-evaporating HNO_3 product from an acidic aerosol would interfere with the N_2O_5 measurement as shown in our previous study (Gržinić et al., 2014). We therefore performed the experiments presented here with neutral sodium sulfate and sodium nitrate aerosol to avoid this interference.

2. Experimental section

A detailed description of the experimental method and setup can be found in our previous publications relating to the production of ^{13}N labeled N_2O_5 (Gržinić et al., 2014) and uptake of N_2O_5 on citric acid aerosol (Gržinić et al., 2015). Here we will present a very cursory description of the ^{13}N production method and the changes that have been implemented to the experimental setup for the present uptake measurements.

The ^{13}N short lived radioactive tracer ($T_{1/2} \approx 10 \text{ min.}$) is produced via the $^{16}\text{O}(\text{p},\alpha)^{13}\text{N}$ reaction in a gas target by irradiating a 20% O_2 in He flow with 11 MeV protons produced by the Injector II cyclotron at the Paul Scherrer Institute, Switzerland. The highly oxidized ^{13}N labeled species are reduced to ^{13}NO for transport via a 580 m long PVDF capillary tube to the laboratory. Figure 1 shows a schematic of the experimental setup used in this study. ^{13}NO containing gas from the accelerator facility (50 ml/min) is mixed with $\sim 3 \text{ ml/min}$ of 10 ppmv non-labeled NO in N_2 from a certified gas cylinder and nitrogen carrier gas (only a very small fraction of NO is labeled with ^{13}N , about 10^{-6} and lower). This gas flow is mixed in the N_2O_5 synthesis reactor with a 50 ml/min flow containing $\sim 8 \text{ ppmv}$ O_3 produced by irradiating a 10% O_2 in N_2 gas mixture with 185nm UV light. The reactor is a glass tube of 34 cm length and 4 cm inner diameter, lined with PTFE foil and operated under dry conditions to minimize hydrolysis of N_2O_5 .

on the walls. The gas phase chemistry of NO with O₃ results in the formation of NO₂, NO₃ and finally N₂O₅ (R1). The resulting gas flow is mixed with a secondary gas flow containing aerosol (720 ml/min) in an aerosol flow tube. This flow tube differs from the one that we used in our previous studies in that it is optimized for measurement of uptake coefficients in the 10⁻¹-10⁻² range. It consists of a glass tube 39.3 cm in length and 1.4 cm in inner diameter. The inside of the glass tube is coated with halocarbon wax to minimize N₂O₅ losses to the wall by heterogeneous hydrolysis. A PTFE tube (6 mm diameter) is inserted coaxially into the flow tube to act as injector for the N₂O₅ flow. The injector contains holes at the end which allow the N₂O₅ flow to be injected perpendicularly to the aerosol flow. Mixing is assumed to be rapid, and a laminar flow profile is assumed to have been established in the first few cm. A black shroud is used to cover the N₂O₅ synthesis reactor and the aerosol flow tube in order to prevent NO₃ photolysis and thus N₂O₅ loss. Aerosol is produced by nebulizing 0.1% wt. NaNO₃, Na₂SO₄ and 1:1 NaNO₃/Na₂SO₄ solutions in MilliQ water. The resulting aerosol flow is dried over a Nafion membrane diffusion drier (RH of the drying gas outside is adjusted to 40% RH to prevent efflorescence), passed through an ⁸⁵Kr bipolar ion source and an electrostatic precipitator to equilibrate the charge distribution and subsequently remove the charged particles, respectively. A humidifier is placed after the ion source to adjust the humidity of the gas flow to the required experimental levels. The overall gas flow exiting from the aerosol fast-flow reactor is split into two flows via a T-connector, one to an SMPS (Scanning Mobility Particle Sizer) system used to characterize the aerosol, consisting of a ⁸⁵Kr bipolar ion source to re-establish charge equilibrium, a differential mobility analyzer (DMA, TSI 3071) and a condensation particle counter (CPC, TSI 3022). The other part of the gas flow is directed into a parallel plate diffusion denuder system, where the various ¹³N containing gaseous species (N₂O₅, NO₃ and NO₂) are trapped by lateral diffusion and chemical reaction on a series of parallel, selectively coated aluminum plates: citric acid for trapping N₂O₅ and NO₃, a 1:1 mixture of NDA (N-(1-naphthyl) ethylene diamine dihydrochloride) and KOH for trapping NO₂. The aerosol particles, which have small diffusivity, pass without loss through the denuder system and are trapped on a glass fiber filter placed at the exit. The radioactive decay of ¹³N is measured by placing a CsI scintillator crystal with PIN diode detectors (Caroll and Ramsey, USA) on each of the denuder traps and the particle filter. ¹³N decays by β^+ decay and the resulting positron annihilates with an electron with emission of two coincident γ -rays in opposite directions. The resulting signal can be related to the concentration of the species in the gas and particle phase by comparing the NO₂ concentration measured with a NO_x analyzer to the ¹³NO₂ and ¹³N₂O₅ signals on the denuder plates and particle filter, respectively. The gas-phase non-labeled NO₂ and N₂O₅ concentrations were around 10¹¹ molecule cm⁻³. The signal on the particle filter is related to aerosol phase nitrate after removal of dissolved N₂O₅ by stripping the gas phase N₂O₅ in the denuder system. The equilibrium established by R4 and R5 is fast enough to ensure that. In turn, the amount of dissolved N₂O₅ remains orders of magnitude smaller than the amount of nitrate built up in the particle phase along the flow tube, so that the net loss of N₂O₅ in the gas phase corresponds to the net gain of nitrate in the particle phase. Unfortunately, due to experimental limitations, only a limited number of measurements could be performed. The ¹³N tracer technique is dependent on smooth operation of the accelerator facilities and constant online ¹³N production to be successful, which is not always the case. Individual experiments involved the acquisition of datapoints consisting of 15-20 activity measurements, each integrated over 60 s, for a given injector position. Overall, replicates from several different experiment series performed on several different operation days of the ¹³N delivering facility were averaged to obtain values and standard deviations reported in Table 1.

3. Results and Discussion

The measurements were performed at 50% and 70% RH for all three of the solutions in question. The operating procedure is similar to the one reported by Gržinić et al. (Gržinić et al., 2015; Gržinić et al., 2014), although in this case the experiment was performed by measuring the change in signals under variation of the position of the injector (reaction time) and not aerosol surface

to volume ratio. Appropriate corrections have been applied to the N_2O_5 signal to account for NO_2 interference on the denuder coating used for N_2O_5 (citric acid) as well as for the small amounts of NO_3 present in the gas phase, as described in our previous studies. Before each experimental run a wall loss measurement was performed without aerosol by moving the injector in 5-10 cm steps along the length of the aerosol flow tube and measuring the gas phase N_2O_5 signal, in order to obtain the pseudo-first order wall loss rate constants (k_w) for each experiment. These values varied between $\sim 3 \times 10^{-2}$ and $\sim 7 \times 10^{-2} \text{ s}^{-1}$, depending on humidity. The citric acid coating used to trap N_2O_5 in the denuder system is not able to differentiate N_2O_5 from HNO_3 . Though, any significant presence of HNO_3 formed along the walls upstream of the aerosol flow tube would have been noticed due to its very large wall loss rate coefficient (Guimbaud et al., 2002), which was not observed; the uptake coefficient for labelled N_2O_5 on the reactor walls calculated from k_w was in the range of 10^{-7} , which would not lead to substantial HNO_3 production. NO_2 concentrations in the system were measured by switching a NO_x analyzer in place of the SMPS system at the beginning of the experiment. By comparing this result to the signals from ^{13}N labelled N_2O_5 and NO_2 , the concentration of non-labelled N_2O_5 in the system was also calculated, as described in our previous studies (Gržinić et al., 2015; Gržinić et al., 2014). The uptake measurements were performed in a similar fashion to the wall loss measurements, although in this case aerosol was introduced at each step. By using Eq. 3, which describes gas-aerosol phase interaction kinetics, we can estimate the uptake coefficient.

$$\frac{C_p^*(t)}{C_g^*(t=0)} = \frac{1 - e^{-(k_w + k_p)t}}{1 + \frac{k_w}{k_p}} \quad (3)$$

$$k_p = \frac{S_p \omega \gamma_{\text{eff}}^*}{4} \quad (4)$$

where $C_g^*(t=0)$ is the gas-phase labelled N_2O_5 concentration in molecules cm^{-3} at time zero, $C_p^*(t)$ is the labelled particle phase nitrate concentration expressed as number of particle phase labelled nitrate ions per volume of gas phase, in ions cm^{-3} , k_w is the wall loss constant, measured as described above, and k_p denotes the apparent first order rate constant for gas-phase loss of labelled N_2O_5 to the aerosol phase, which can be related to the effective uptake coefficient (γ_{eff}^*) of labelled N_2O_5 by Equation 4, where S_p is the total aerosol surface area to gas volume ratio of the aerosol and ω is the mean thermal velocity of N_2O_5 . Figure 2 shows the appearance of ^{13}N in the aerosol phase as a function of time performed together with least-squares fits using Eq. (3) with γ_{eff}^* as the only variable. The true uptake coefficients were then obtained by correction for gas phase diffusion of N_2O_5 , as described by Pöschl et al. (2007), which leads to considerable corrections for uptake coefficients above 0.1 and particle diameters around 400 nm. The diffusion coefficient was taken as $0.085 \text{ cm}^2 \text{ s}^{-1}$ at ambient temperature and pressure (Tang et al., 2014). Table 1 shows the results obtained for the various aerosols, with corresponding experimental parameters, including γ_{eff}^* as returned from the fits to the data and γ^* after the diffusion correction. In absence of aerosol phase nitrate, the obtained γ^* for Na_2SO_4 at 70% RH is comparable to that reported by Mentel et al. (1999). At 50% RH, it is likely that the Na_2SO_4 particles remained effloresced (Gao et al., 2007) (the lowest RH in the aerosol conditioning system was 40%), explaining the low γ of 0.0053, which is comparable to that previously reported for dry ammonium sulfate (Hallquist et al., 2003). In presence of aerosol phase nitrate, uptake of ^{13}N -labelled N_2O_5 is drastically higher than the net uptake of non-labelled N_2O_5 observed in earlier studies by (Bertram and Thornton, 2009; Griffiths et al., 2009; Hallquist et al., 2003; Mentel et al., 1999; Wahner et al., 1998) or that predicted by the IUPAC recommended expression also included in the table. A strong dependence of γ^* on humidity is observed, with an increase by a factor about three from 50% to 70% relative humidity. On mixed $\text{Na}_2\text{SO}_4 / \text{NaNO}_3$ aerosol, the uptake is very close to that of pure NaNO_3 aerosol, at both humidities. Since the measured uptake coefficient for ^{13}N labelled N_2O_5 into the nitrate containing aerosol is about an order of magnitude larger than any uptake coefficient measured into not strongly acidic aqueous aerosol in previous studies, our results

demonstrate that gas – aqueous phase exchange of N_2O_5 at room temperature and its dissociation are very efficient, as also suggested by Mentel et al. (1999), based on experiments with NaNO_3 , Na_2SO_4 and NaHSO_4 aerosol.

More insight into the interpretation of the present experiments with ^{13}N labeled N_2O_5 can be obtained by deconvoluting the chemical mechanism of N_2O_5 hydrolysis (R3-7) to take into account the fate of the labelled and non-labelled species separately. Assuming that the labeled N_2O_5 molecules contain only one ^{13}N atom (due to the very low labeled to non-labeled NO ratio of around 10^{-6}) and under the assumption that no isotopic effects are in play, the chemical mechanism can be assumed to proceed as shown in Figure 3a. We first assume that upon dissociation of $^{13}\text{NNO}_5$, there is an equal possibility that the ^{13}N label will end up either in the nitronium ion (NO_2^+) or in the nitrate ion (NO_3^-), with rate coefficients $k_4/2$. In the first scenario (right branch of the pathway for ' N^*NO_5 ' in Fig. 3a) the ^{13}N label ends up on the nitrate ion (R4''). The corresponding non-labelled nitronium ion, if not reacting with H_2O , R7, reacts with the excess non-labelled nitrate to form non-labelled N_2O_5 (R5), while only a negligible fraction reacts with the labeled $^{13}\text{NO}_3^-$ (R5'') and thus most of the labeled $^{13}\text{NO}_3^-$ is lost in the excess nitrate pool present in the aerosol. N_2O_5 re-evaporating to the gas phase is therefore non-labeled. Thus, in this branch, all ^{13}N labels remain in the aqueous phase given that evaporation as HNO_3 is unlikely for our neutral aerosol. As evident from the experiments, the net transfer of labelled N_2O_5 into the aerosol nitrate pool, and thus the combination of bulk accommodation and dissociation, is very fast.

In the other scenario (left branch of ' N^*NO_5 ' pathway in Fig. 3a) of the mechanism, ^{13}N ends up on the nitronium ion (R4'), and there are two possibilities for its further fate. The $^{13}\text{NO}_2^+$ can react with water (R7'), bringing the label into the particulate nitrate pool. Alternatively $^{13}\text{NO}_2^+$ can react with NO_3^- from the nitrate pool (R5') to reform $^{13}\text{NNO}_5$ which can eventually re-evaporate. Obviously which of these two sub-channels are prevalent depends on water and nitrate concentrations as well as the rate coefficients of the two competing reactions. The water and nitrate concentrations for the conditions of the present experiments were derived from the AIM model (Clegg et al., 1998) and are also listed in Table 1. In presence of nitrate, (R5') is the dominant pathway, as shown by Mentel et al. (1999) and Wahner et al. (1998), where values for the ratio k_5/k_7 of around 900 and 260, respectively, had been used as fitting parameters to explain the entirety of the nitrate effect.

In Figure 3b, we report the results of box model calculations (described in the supporting information) for the scheme shown in Figure 3a to substantiate these effects for NaNO_3 aerosol at 70% RH. We have used the rate coefficients for $k_4 = 5 \times 10^6 \text{ s}^{-1}$, $k_5 = 2.4 \times 10^{10} \text{ M}^{-1} \text{ s}^{-1}$ and $k_7 = 2.6 \times 10^7 \text{ M}^{-1} \text{ s}^{-1}$ as suggested by Mentel et al. (1999) for NaNO_3 aerosol at various humidities; the bulk accommodation coefficient α_b was set to one. Figure 3b (left y-axis) directly demonstrates the rapid removal of labelled nitrogen from aqueous phase N_2O_5 and its appearance as labelled nitrate. Parallel to that, labelled N_2O_5 disappears much more quickly from the gas phase and appears as aerosol phase nitrate than non labelled N_2O_5 , as shown in Figure 3d. It is also instructive to look at the rates of individual reactions contributing to the aqueous phase budget of labelled species plotted in Figure 3b and those of the non-labelled species in Figure 3c: Even though R5' brings back half of the labelled N_2O_5 (rate of R5' is half of the dissociation rate, Figure 3b), the fraction of labelled N_2O_5 drops below half of its initial value, since the exchange reactions R4 and R5 are fast, so that it may cycle through the aqueous phase part of the scheme many times. The rate of R5'' (labelled nitrate with non-labelled nitronium) is not getting competitive, so that labelled nitrate remains in the nitrate pool. The γ^* values calculated from the net N_2O_5 loss rates are about 0.26 for labelled N_2O_5 , in good agreement with the value observed in the experiment, 0.29, and 0.0033 for non-labelled N_2O_5 . The latter is consistent with the observation by Mentel et al. but lower than that suggested by the parameterization given in equation (1) based on the IUPAC recommendation and listed in Table 1 or that suggested by Bertram and Thornton (2009) or Griffiths et al. (2009) developed based on a wider data set with other aerosol compositions. Box model simulation of the mixed salt case (not shown), also at 70% RH, returns essentially the same results, 0.25 and 0.009, for the uptake coefficient of labelled and non-labelled N_2O_5 , respectively, also in line with our measured γ^* of 0.26 for labelled N_2O_5 . The right column of Figure 3, plots e,f,g,h, present the box model results for Na_2SO_4 aerosol at 70% RH. The main difference is that in this case, R5 represents

only a negligible pathway for non-labelled nitronium resulting from R4", so that the majority of labelled nitrate recycles back to labelled N_2O_5 via R5". As a result, both labelled and non-labelled species behave exactly parallel, both in terms of rates and concentration. When solubility and rate coefficient are taken the same as those for the nitrate aerosol, the magnitude of the calculated uptake coefficient is an order of magnitude too high. The difference between the kinetics described by Mentel et al. (1999) and Bertram and Thornton (2009) is that overall uptake is limited by the dissociation, k_4 , in the latter, while Mentel et al. suggest faster dissociation and limitation by the interplay of the reactions of NO_2^+ with H_2O and NO_3^- . Replacing k_4 by the parameterization suggested by Bertram and Thornton, keeping k_5 as before, but replacing k_7 such that $k_7/k_5=0.06$ as suggested by Bertram and Thornton, yields $\gamma = 0.06$, in reasonable agreement with the uptake coefficient measured here (0.027). However, this can as well be achieved by the Mentel et al. kinetics scheme via lowering k_7 by one order of magnitude to achieve lower net uptake, which is what has been used in the calculations shown in Figure 3f,g,h. In view of the limited dataset it has been beyond the scope of this study to retrieve more precise rate coefficients for R4, R5 and R7. The present results clearly indicate that accommodation and dissociation of N_2O_5 are not limiting net uptake for aerosol containing substantial amounts of nitrate. Furthermore, these experiments provide direct evidence that these elementary steps actually exist, because otherwise exchange with the non-labelled nitrate pool would not occur.

The measured uptake coefficient increases with RH (water content) as the increase in water concentration promotes the reaction of $^{13}\text{NO}_2^+$ with water (R7') while at the same time a decrease in nitrate concentration suppresses the $^{13}\text{NNO}_5$ reformation sub-channel (R5'). However, as argued above, in presence of nitrate at several M, the dominant fate of the label in the left branch of the mechanism in Fig. 3a is the reformation of labeled N_2O_5 . If bulk accommodation would limit uptake, the measured uptake coefficient would be only slightly larger than $\alpha_b/2$, with $\alpha_b/2$ contributed by the right branch of the mechanism, and a minor contribution from the left branch. Our results therefore strongly indicate that α_b must be at least about twice as high as the uptake coefficient of ^{13}N -labelled N_2O_5 measured for NaNO_3 and $\text{NaNO}_3/\text{Na}_2\text{SO}_4$ aerosols and thus $\alpha_b>0.4$ when including the uncertainties related to aerosol surface to volume ratio and correction for gas phase diffusion. In the box model simulations discussed above, α_b has been set to one. The only systematic uncertainty not considered in this is the assumption that isotope effects do not influence the symmetry of the disproportionation reaction (R4).

Interestingly, the measured uptake coefficient is more sensitive to the water activity, irrespective of whether it is pure nitrate or mixed nitrate / sulfate particles, than to the fractional nitrate content. In spite of the fact that the expected ratio $k_7[\text{H}_2\text{O}]/k_5[\text{NO}_3^-]$ (see Table 1) increases substantially from pure nitrate to mixed nitrate / sulfate, still bulk accommodation and dissociation are not limiting, and the efficient exchange of the label with the non-labelled nitrate pool dominates the behavior. Thus an increase of α_b , solubility in terms of salting effects, or of the dissociation could explain the increase of the uptake coefficient of labelled N_2O_5 by a factor of four from 50 to 70 % RH.. As discussed first by Mentel et al. (1999), and later by Griffiths et al. (2009) and Bertram and Thornton (2009), the kinetic regime may shift between limitation by R7, R4 or R3 between low and high water activity, and it remains difficult to unambiguously assign the kinetic regime. Also from the present study, the evidence for the fast dissociation is very strong for the high nitrate mole fractions used, and we can only suggest that the dissociation is similarly fast for the salt aerosol in absence of nitrate.

On a side note, in principle, we cannot exclude a surface contribution. Since also the suggested bulk accommodation is followed via obviously very fast dissociation into nitronium and nitrate, this process will occur close to the surface anyhow, with a short reacto-diffusive length (in contrast to the much slower hydrolysis reaction of nitronium with H_2O). Therefore, for instance, varying the surface to volume ratio of the aerosol would not allow differentiating bulk from surface accommodation. Though, we would prefer not invoking a surface process if bulk phase processing explains the observations.

Obviously, the fast isotope exchange that allows tracking the dissociation of dissolved N_2O_5 depends on the presence of a nitrate pool, which has to be substantial enough to ‘trap’ the ^{13}N tracer and prevent its release. In other words, this method traces uptake of N_2O_5 into the non-limiting pool of aqueous nitrate. In absence of nitrate, R7' and R7 dominate in both branches (Fig. 3e), and the measured uptake coefficient for the ^{13}N labelled N_2O_5 is comparable to that reported with other techniques for the same aerosol, in the range of a few 10^{-2} for Na_2SO_4 at 70% RH in this study or for $(\text{NH}_4)_2\text{SO}_4$ reported by Gržinić et al. (2014), both consistent with available literature. For comparison, calculated uptake coefficients based on the parameterization and values from the IUPAC evaluation (Ammann et al., 2013), implemented in equation (1) and (2), are also listed in Table 1.

Conclusion and atmospheric implications

Highly efficient uptake of ^{13}N -labelled N_2O_5 into nitrate containing aqueous aerosol was observed and attributed to the exchange of ^{13}N labeled nitrate as dissociation product of N_2O_5 with the nitrate pool in the aqueous phase. This allows suggesting a very large value for the bulk mass accommodation coefficient for N_2O_5 into an aqueous aerosol at room temperature of $\alpha_b > 0.4$ at high relative humidity and fast dissociation at $> 10^6 \text{ s}^{-1}$. This also provides direct evidence that the fast dissociation into nitrate and nitronium at $> 10^6 \text{ s}^{-1}$ actually occurs, and thus also supports the arguments behind the nitrate effect. The observed behavior of ^{13}N -labelled N_2O_5 is similar to that observed by Wachsmuth et al. (2002), where $^{83-86}\text{Br}$ isotopes have been used to determine the bulk accommodation coefficient of HOBr on aqueous bromide containing aerosol. The large value of α_b obtained for N_2O_5 at room temperature implies that other limiting processes must be at work to explain the insensitivity of the uptake coefficient to water content at high relative humidity (Abbatt et al., 2012; Griffiths et al., 2009; Thornton et al., 2003). Possible other aspects may be the temperature dependence of the solubility of N_2O_5 or salting effects as discussed in these previous studies, for which also strong indications come from this study to explain the strong water activity dependence of the observed uptake coefficient of ^{13}N labelled N_2O_5 . At least this study would exclude any accommodation limitation and supports previous indications that reaction and diffusion limit uptake of N_2O_5 to low viscosity aqueous aerosol (Gaston and Thornton, 2016).

Acknowledgements

The authors would like to thank the staff of the PSI accelerator facilities and of the isotope production facility IP-2 for their invaluable help during experimental work. Technical support by M. Birrer is much appreciated. This study was supported by the Swiss National Science Foundation (grants no. 130175 and 149492).

The Supplement related to this article is available online

References

Abbatt, J. P. D., Lee, A. K. Y., and Thornton, J. A.: Quantifying trace gas uptake to tropospheric aerosol: recent advances and remaining challenges, *Chem. Soc. Rev.*, 41, 6555-6581, doi: 10.1039/C2CS35052A, 2012.

Ammann, M.: Using ^{13}N as tracer in heterogeneous atmospheric chemistry experiments, *Radiochim. Acta*, 89, 831-838, 2001.

Ammann, M., Cox, R. A., Crowley, J. N., Jenkin, M. E., Mellouki, A., Rossi, M. J., Troe, J., and Wallington, T. J.: Evaluated kinetic and photochemical data for atmospheric chemistry: Volume VI – heterogeneous reactions with liquid substrates, *Atmos. Chem. Phys.*, 13, 8045-8228, doi: 10.5194/acp-13-8045-2013, 2013.

Anttila, T., Kiendler-Scharr, A., Tillmann, R., and Mentel, T. F.: On the reactive uptake of gaseous compounds by organic-coated aqueous aerosols: Theoretical analysis and application to the heterogeneous hydrolysis of N_2O_5 , *J. Phys. Chem. A*, 110, 10435-10443, 2006.

Badger, C. L., Griffiths, P. T., George, I., Abbatt, J. P. D., and Cox, R. A.: Reactive uptake of N_2O_5 by aerosol particles containing mixtures of humic acid and ammonium sulfate, *J. Phys. Chem. A*, 110, 6986-6994, 2006.

Behnke, W., George, C., Scheer, V., and Zetzsch, C.: Production and decay of ClNO_2 , from the reaction of gaseous N_2O_5 with NaCl solution: Bulk and aerosol experiments, *J. Geophys. Res.*, 102, 3795-3804, doi: 10.1029/96jd03057, 1997.

Bertram, T. H. and Thornton, J. A.: Toward a general parameterization of N_2O_5 reactivity on aqueous particles: the competing effects of particle liquid water, nitrate and chloride, *Atmos. Chem. Phys.*, 9, 8351-8363, 2009.

Bertram, T. H., Thornton, J. A., Riedel, T. P., Middlebrook, A. M., Bahreini, R., Bates, T. S., Quinn, P. K., and Coffman, D. J.: Direct observations of N_2O_5 reactivity on ambient aerosol particles, *Geophys. Res. Lett.*, 36, 2009.

Chang, W. L., Bhave, P. V., Brown, S. S., Riemer, N., Stutz, J., and Dabdub, D.: Heterogeneous Atmospheric Chemistry, Ambient Measurements, and Model Calculations of N_2O_5 : A Review, *Aerosol Sci. Technol.*, 45, 665-695, doi: 10.1080/02786826.2010.551672, 2011.

Clegg, S. L., Brimblecombe, P., and Wexler, A. S.: Thermodynamic model of the system $\text{H}^+ \text{-NH}_4^+ \text{-Na}^+ \text{-SO}_4^{2-} \text{-NO}_3^- \text{-Cl}^- \text{-H}_2\text{O}$ at 298.15 K, *J. Phys. Chem. A*, 102, 2155-2171, 1998.

Dentener, F. J. and Crutzen, P. J.: Reaction of N_2O_5 on tropospheric aerosols: Impact on the global distributions of NO_x , O_3 , and OH , *J. Geophys. Res.*, 98, 7149-7163, doi: 10.1029/92JD02979, 1993.

Evans, M. J. and Jacob, D. J.: Impact of new laboratory studies of N_2O_5 hydrolysis on global model budgets of tropospheric nitrogen oxides, ozone, and OH, *Geophys. Res. Lett.*, 32, 2005.

Folkers, M., Mentel, T. F., and Wahner, A.: Influence of an organic coating on the reactivity of aqueous aerosols probed by the heterogeneous hydrolysis of N_2O_5 , *Geophys. Res. Lett.*, 30, 2003.

Gaston, C. J. and Thornton, J. A.: Reacto-Diffusive Length of N_2O_5 in Aqueous Sulfate- and Chloride-Containing Aerosol Particles, *J. Phys. Chem. A*, 120, 1039-1045, doi: 10.1021/acs.jpca.5b11914, 2016.

Gao Y., Yu L.E., and Chen S.B., Efflorescence Relative Humidity of Mixed Sodium Chloride and Sodium Sulfate Particles, *J. Phys. Chem. A*, 111, 10660–10666, 2007.

George, C., Ponche, J. L., Mirabel, P., Behnke, W., Scheer, V., and Zetzsch, C.: Study of the Uptake of N_2O_5 by Water and NaCl Solutions, *J. Phys. Chem.*, 98, 8780-8784, 1994. Griffiths, P. T., Badger, C. L., Cox, R. A., Folkers, M., Henk, H. H., and Mentel, T. F.: Reactive Uptake of N_2O_5 by Aerosols Containing Dicarboxylic Acids. Effect of Particle Phase, Composition, and Nitrate Content, *J. Phys. Chem. A*, 113, 5082-5090, 2009.

Gross, S., Iannone, R., Xiao, S., and Bertram, A. K.: Reactive uptake studies of NO_3 and N_2O_5 on alkenoic acid, alkanoate, and polyalcohol substrates to probe nighttime aerosol chemistry, *Phys. Chem. Chem. Phys.*, 11, 7792-7803, 2009.

Gržinić, G., Bartels-Rausch, T., Berkemeier, T., Türler, A., and Ammann, M.: Viscosity controls humidity dependence of N_2O_5 uptake to citric acid aerosol, *Atmos. Chem. Phys.*, 15, 13615-13625, doi: 10.5194/acp-15-13615-2015, 2015.

Gržinić, G., Bartels-Rausch, T., Birrer, M., Türler, A., and Ammann, M.: Production and use of ^{13}N labeled N_2O_5 to determine gas-aerosol interaction kinetics, *Radiochimica Acta*, 102, 1025–1034, doi: 10.1515/ract-2014-2244, 2014.

Guimbaud, C., Arens, F., Gutzwiller, L., Gäggeler, H. W., and Ammann, M.: Uptake of HNO_3 to deliquescent sea-salt particles: a study using the short-lived radioactive isotope tracer N-13, *Atmos. Chem. Phys.*, 2, 249-257, 2002.

Hallquist, M., Stewart, D. J., Stephenson, S. K., and Cox, R. A.: Hydrolysis of N_2O_5 on sub-micron sulfate aerosols, *Phys. Chem. Chem. Phys.*, 5, 3453-3463, 2003.

Hanson, D. R. and Lovejoy, E. R.: The Uptake of N_2O_5 onto Small Sulfuric-Acid Particles, *Geophys. Res. Lett.*, 21, 2401-2404, 1994.

Karagulian, F., Santschi, C., and Rossi, M. J.: The heterogeneous chemical kinetics of N_2O_5 on CaCO_3 and other atmospheric mineral dust surrogates, *Atmos. Chem. Phys.*, 6, 1373-1388, 2006.

Mentel, T. F., Sohn, M., and Wahner, A.: Nitrate effect in the heterogeneous hydrolysis of dinitrogen pentoxide on aqueous aerosols, *Phys. Chem. Chem. Phys.*, 1, 5451-5457, 1999.

Mozurkewich, M. and Calvert, J. G.: Reaction probability of N_2O_5 on aqueous aerosols, *J. Geophys. Res.*, 93, 15889-15896, doi: 10.1029/JD093iD12p15889, 1988.

Phillips, G. J., Thieser, J., Tang, M., Sobanski, N., Schuster, G., Fachinger, J., Drewnick, F., Borrmann, S., Bingemer, H., Lelieveld, J., and Crowley, J. N.: Estimating N_2O_5 uptake coefficients using ambient measurements of NO_3 , N_2O_5 , ClNO_2 and particle-phase nitrate, *Atmos. Chem. Phys.*, 16, 13231-13249, doi: 10.5194/acp-16-13231-2016, 2016.

Pöschl, U., Rudich, Y., and Ammann, M.: Kinetic model framework for aerosol and cloud surface chemistry and gas-particle interactions - Part 1: General equations, parameters, and terminology, *Atmos. Chem. Phys.*, 7, 5989-6023, 2007.

Tang, M. J., Cox, R. A., and Kalberer, M.: Compilation and evaluation of gas phase diffusion coefficients of reactive trace gases in the atmosphere: volume 1. Inorganic compounds, *Atmos. Chem. Phys.*, 14, 9233-9247, 2014.

Thornton, J. A. and Abbatt, J. P. D.: N_2O_5 reaction on submicron sea salt aerosol: Kinetics, products, and the effect of surface active organics, *J. Phys. Chem. A*, 109, 10004-10012, 2005.

Thornton, J. A., Braban, C. F., and Abbatt, J. P. D.: N_2O_5 hydrolysis on sub-micron organic aerosols: the effect of relative humidity, particle phase, and particle size, *Phys. Chem. Chem. Phys.*, 5, 4593-4603, 2003.

Wachsmuth, M., Gäggeler, H. W., von Glasow, R., and Ammann, M.: Accommodation coefficient of HOBr on deliquescent sodium bromide aerosol particles, *Atmos. Chem. Phys.*, 2, 121-131, doi: 10.5194/acp-2-121-2002, 2002.

Wagner, C., Hanisch, F., Holmes, N., de Coninck, H., Schuster, G., and Crowley, J. N.: The interaction of N_2O_5 with mineral dust: aerosol flow tube and Knudsen reactor studies, *Atmos. Chem. Phys.*, 8, 91-109, 2008.

Wagner, N. L., Riedel, T. P., Young, C. J., Bahreini, R., Brock, C. A., Dubé, W. P., Kim, S., Middlebrook, A. M., Öztürk, F., Roberts, J. M., Russo, R., Sive, B., Swarthout, R., Thornton, J. A., VandenBoer, T. C., Zhou, Y., and Brown, S. S.: N_2O_5 uptake coefficients and nocturnal NO_2 removal rates determined from ambient wintertime measurements, *J. Geophys. Res.*, 118, 9331-9350, doi: 10.1002/jgrd.50653, 2013.

Wahner, A., Mentel, T. F., Sohn, M., and Stier, J.: Heterogeneous reaction of N_2O_5 on sodium nitrate aerosol, *J. Geophys. Res.*, 103, 31103-31112, 1998.

Table 1. Experimental parameters and results

Aerosol	NaNO ₃	NaNO ₃	NaNO ₃ / Na ₂ SO ₄	NaNO ₃ / Na ₂ SO ₄	Na ₂ SO ₄	Na ₂ SO ₄
Molar mixing ratio	-	-	1:1	1:1	-	-
Temperature (K)	295±1	295±1	295±1	295±1	295±1	295±1
RH (%)	50±1	70±1	51±1	70±1	51±1	70±1
Average S/V ratio (m ² /m ³)	5.66×10 ⁻³	5.00×10 ⁻³	3.36×10 ⁻³	4.76×10 ⁻³	3.42×10 ⁻³	3.00×10 ⁻³
$\gamma^*_{\text{eff}}(^{13}\text{NNO}_5)$	0.057	0.18	0.054	0.17	0.0052	0.025
Error ^a	±0.004	±0.02	±0.008	±0.02	±0.002	±0.003
$\gamma^* (^{13}\text{NNO}_5)$ ^b	0.067	0.29	0.063	0.26	0.0053	0.027
Total error ^c	±0.02	±0.1	±0.02	±0.2	±0.002	±0.008
[H ₂ O] (M) ^d	28.5	38.2	34.4	41.6	38.6	43.8
[NO ₃ ⁻] (M) ^d	13.1	8.78	4.60	3.29	0	0
$k_7[\text{H}_2\text{O}] / k_5[\text{NO}_3^-]$ ^e	0.044	0.087	0.15	0.25	-	-
γ (non-labelled N ₂ O ₅) ^f	0.0050	0.010	0.013	0.019	0.044	0.047

^a 95% confidence level of the fit of eq. (3) to the data as shown in Fig. 2^b corrected for diffusion in the gas phase^c including 30% uncertainty related to the aerosol surface to volume ratio^d from AIM model (Clegg et al., 1998)^e $k_7/k_5 = 0.02$ ^f calculated using equations (1) and (2), with $k_0^{\text{II}} = 10^5 \text{ M}^{-1} \text{ s}^{-1}$ and $H = 2 \text{ M atm}^{-1}$

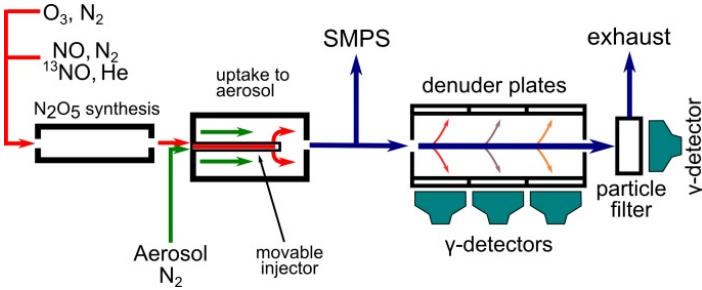


Fig. 1. Schematic of the modified experimental setup used in this study

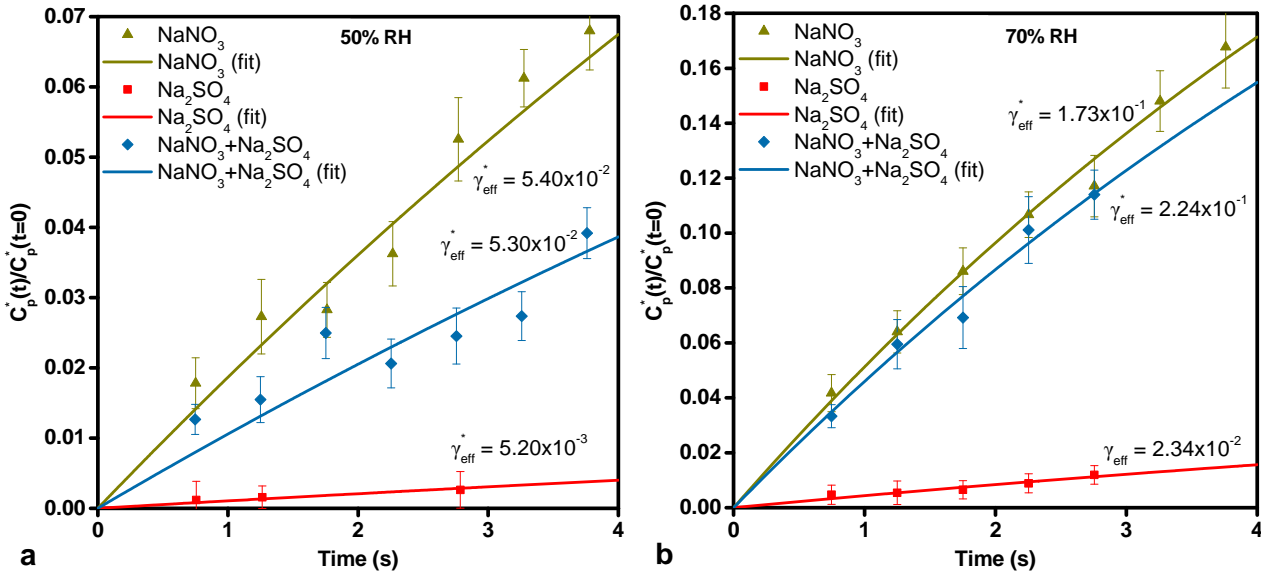


Fig. 2. Normalized particle-phase labelled nitrate concentration vs. time graph for experiments performed at 50% RH (a) and 70% RH (b). The data points represent the measurement data, the error bars represent the standard deviation of the measurements, the curves are a least-squares fit of Eq. 1 to the measured data.

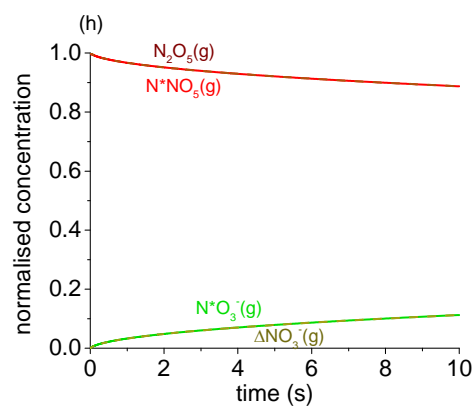
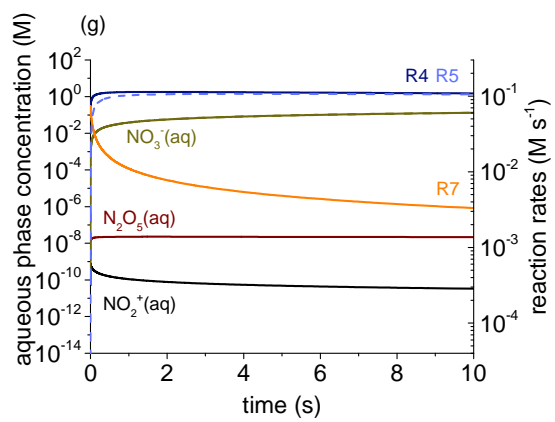
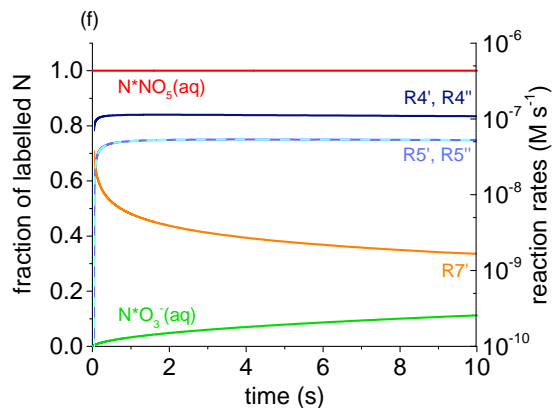
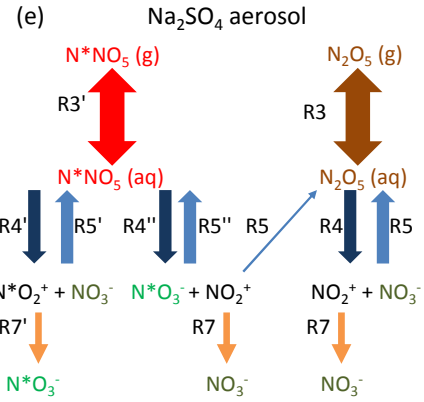
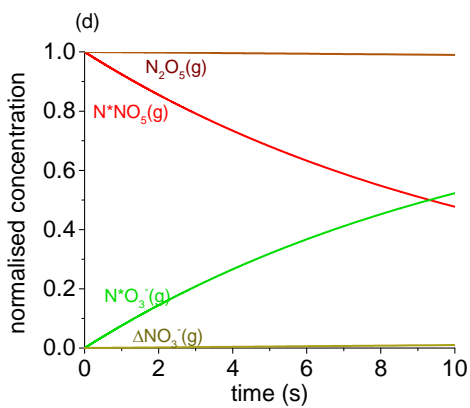
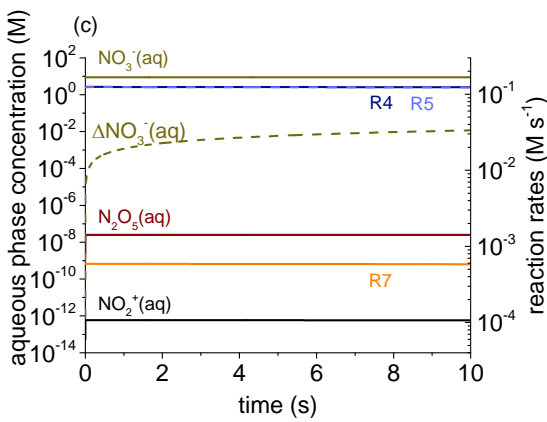
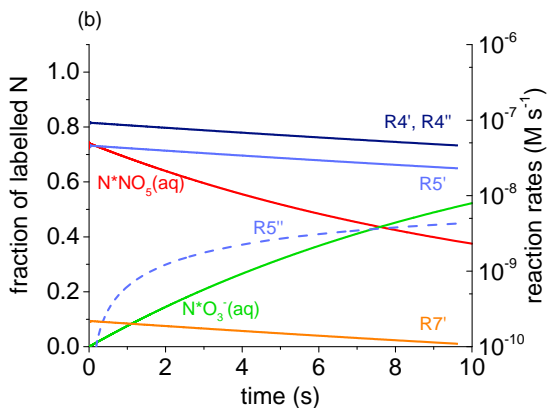
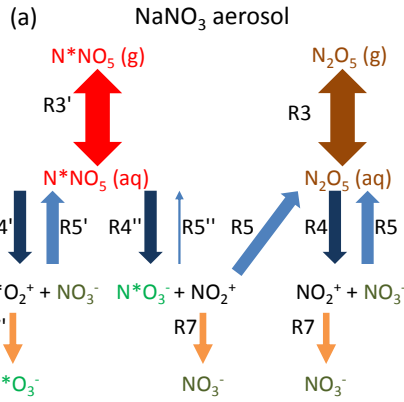


Fig. 3. (a) The chemical mechanism of N_2O_5 hydrolysis and chemical isotope exchange in nitrate containing solutions. N^* refers to ^{13}N . (b, c, d) Results of box model calculations for NaNO_3 aerosol at 70% RH: evolution as a function of time of: (b) the fraction of labelled N_2O_5 in the aqueous phase (red, left axis) and ratio of labelled nitrate to the total number of labeled N_2O_5 initially available (green, left axis); rates of reactions relevant for the budget of aqueous phase ^{13}N (light to dark blue, right axis); (c) rates of reactions relevant for the budget of non-labelled species in the aqueous phase; (d) evolution of normalized gas phase N_2O_5 (labelled, red; non-labelled, brown) and aqueous phase nitrate (labelled, green; non-labelled, olive) as a function of time. (e, f, g, h) scheme and plots of the same quantities, but for Na_2SO_4 aerosol at 70% RH in absence of pre-existing nitrate.